

# Actin–Curcumin Interaction: Insights into the Mechanism of Actin Polymerization Inhibition

Gopa Dhar,<sup>†</sup> Devlina Chakravarty,<sup>†</sup> Joyita Hazra,<sup>‡</sup> Jesmita Dhar,<sup>§</sup> Asim Poddar,<sup>†</sup> Mahadeb Pal,<sup>‡</sup> Pinak Chakrabarti,<sup>†</sup> Avadhesh Surolia,<sup>\*,||</sup> and Bhabatarak Bhattacharyya<sup>\*,†</sup>

<sup>†</sup>Department of Biochemistry, Bose Institute, Kolkata 700054, India

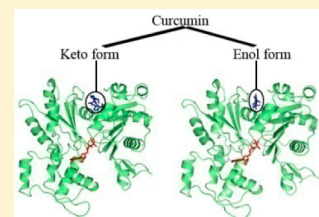
<sup>‡</sup>Division of Molecular Medicine, Bose Institute, Kolkata 700054, India

<sup>§</sup>Bioinformatics Centre, Bose Institute, Kolkata 700054, India

<sup>||</sup>Molecular Biophysics Unit, Indian Institute of Science, Bangalore 560012, India

## Supporting Information

**ABSTRACT:** Curcumin, derived from rhizomes of the *Curcuma longa* plant, is known to possess a wide range of medicinal properties. We have examined the interaction of curcumin with actin and determined their binding and thermodynamic parameters using isothermal titration calorimetry. Curcumin is weakly fluorescent in aqueous solution, and binding to actin enhances fluorescence several fold with a large blue shift in the emission maximum. Curcumin inhibits microfilament formation, which is similar to its role in inhibiting microtubule formation. We synthesized a series of stable curcumin analogues to examine their affinity for actin and their ability to inhibit actin self-assembly. Results show that curcumin is a ligand with two symmetrical halves, each of which possesses no activity individually. Oxazole, pyrazole, and acetyl derivatives are less effective than curcumin at inhibiting actin self-assembly, whereas a benzylidene derivative is more effective. Cell biology studies suggest that disorganization of the actin network leads to destabilization of filaments in the presence of curcumin. Molecular docking reveals that curcumin binds close to the cytochalasin binding site of actin. Further molecular dynamics studies reveal a possible allosteric effect in which curcumin binding at the “barbed end” of actin is transmitted to the “pointed end”, where conformational changes disrupt interactions with the adjacent actin monomer to interrupt filament formation. Finally, the recognition and binding of actin by curcumin is yet another example of its unique ability to target multiple receptors.



Actin is a highly conserved cytoskeletal protein involved in maintaining the integrity of a cell's architecture, mediating signal transduction to regulate cell shape, growth, and motility, and generating mechanical forces within the cell.<sup>1–3</sup> The actin network of eukaryotic cells undergoes drastic changes and remodeling during cell division.<sup>4</sup> Such regulation of the actin cytoskeleton and cell cycle progression appears to be interconnected. Actin and tubulin are contractile proteins that are similar in many respects; they both maintain dynamic equilibrium with their respective polymers inside the cell. These dynamic equilibria control cell division, growth, motility, signaling, and the development and maintenance of cell shape.<sup>5</sup> Tubulin and microtubules are established targets of anticancer drug development.<sup>6,7</sup> The interest in tubulin as a chemotherapeutic target has initiated investigations into the molecular nature of tubulin/drug interactions. There are a significant number of structurally diverse anticancer drugs that function as anti-microtubule agents and possess a common mechanism of action. Surprisingly, no actin-targeted inhibitor has yet been developed as a chemotherapeutic drug for clinical use. Nevertheless, like tubulin, actin also plays an important role in cell division. Moreover, involvement of the actin cytoskeleton has been implicated in the process of apoptotic cell death.<sup>8</sup> It has also been well established that the actin cytoskeleton plays a crucial role in mediating signal trans-

duction between intracellular and extracellular compartments.<sup>9</sup> Recently, work in the field of actin and its regulatory proteins demonstrated that they could be selectively targeted in cancer chemotherapy.<sup>10–12</sup> Experimental data suggest that increased levels of soluble actin and decreased levels of polymerized actin are early events in tumorigenesis.<sup>11</sup> Measurement of the relative levels of the two forms of actin, monomeric and polymeric, in cells might be important for identifying the individuals at risk for certain cancers.<sup>11</sup> A significant number of effective and structurally diverse compounds have been discovered from natural sources that are capable of modulating actin polymerization and dynamics, often through unique mechanisms.<sup>13</sup> Among these molecules, cytochalasins have been extensively studied and act on actin to disrupt filamental organization in cells.<sup>14</sup> In addition, latrunculins, which are natural marine products, can bind to actin and disrupt its organization in a wide variety of cells.<sup>15</sup> These molecules specifically bind to actin filaments, effectively inhibiting cell proliferation.<sup>15</sup> However, it is worth noting that the mechanism of action for many of these drugs is still unknown.

**Received:** November 21, 2014

**Revised:** December 30, 2014

**Published:** January 6, 2015



Curcumin, a major active component of turmeric, is currently in a phase II clinical trial for patients with advanced pancreatic cancer.<sup>16</sup> It inhibits proliferation and induces apoptosis in a wide range of cancer cell types.<sup>17</sup> Surprisingly, unlike most chemotherapeutic agents, curcumin shows no toxicity; it is believed that this unique property of curcumin is due to its cytotoxic activity being confined only to cancer cells.<sup>18,19</sup> Its characterization has revealed a broad range of medicinal utilities, including antiproliferative, anticarcinogenic, anti-inflammatory, antioxidant, antiviral, antifungal, and antimicrobial activities.<sup>18,20</sup> Although most of the conventional chemotherapeutic drugs in use today were designed to recognize a particular target, reports demonstrate either directly or indirectly that curcumin can bind to multiple proteins,<sup>18</sup> transcription factors,<sup>21</sup> coactivators and corepressors, and so forth.<sup>22</sup> To inhibit tumorigenesis, curcumin suppresses oncogenic cell proliferation by inducing apoptosis and arresting cell cycle progression.<sup>23</sup> Earlier, Chen et al. had shown that the effect of curcumin on the viability and induction of apoptosis in the A549 cell line was associated with disorganization of the actin cytoskeleton.<sup>24</sup> They demonstrated that curcumin led to disorganization of actin fibers in combination with induced apoptosis. Recently, Holy has shown effects of curcumin on cell motility and microfilament disorganization using the human prostate cancer cell lines PC-3 and LNCaP.<sup>25</sup>

Curcumin is unstable in aqueous solution at physiological pH, especially in the presence of reducing agents. It decomposes rapidly in the presence of light. The effect of curcumin on actin has mostly been studied in cells. An obvious question is how the decomposed products affect the binding of curcumin to an actin filament or monomer in growing cells. In such cases, it is always desirable to have data from an in vitro purified system. It is also important to know where curcumin binds to actin, and its binding characteristics, thermodynamic parameters, structure–function relationship, and pharmacophoric attachment points to the target, which would aid in designing better analogues. In the present study, we have examined the binding of curcumin to purified actin. To further understand the structure–function relationship of curcumin to actin binding, we synthesized a number of curcumin analogues and examined their binding with actin. Screening of the synthesized analogues has been performed by determining their binding affinities for actin, capacity to inhibit actin self-assembly, and effect on the microfilament network in cells using fluorescence microscopy. In addition, using molecular dynamics, we have tried to focus on the mechanism underlying curcumin-induced inhibition of actin polymerization. We believe that new insights into the mode of actin/curcumin interactions and their structure–function relationship could lead to increased interest in the therapeutic potential of compounds that target the actin cytoskeleton.

## MATERIALS AND METHODS

Curcumin (from *Curcuma longa* or turmeric), rabbit muscle actin ( $\geq 85\%$  (SDS–PAGE), lyophilized powder), adenosine 5'-triphosphate (ATP) disodium salt hydrate, and latrunculin B were obtained from Sigma-Aldrich. Pyrene-labeled actin was purchased from Cytoskeleton, Inc. Rhodamine phalloidin was obtained from Life Technologies. Tris(hydroxymethyl)-aminomethane, magnesium chloride ( $\text{MgCl}_2$ ), potassium chloride (KCl), and calcium chloride ( $\text{CaCl}_2$ ) were purchased from Merck. Buffer solutions were prepared with neat water from a Millipore Milli-Q NANO pure water system. All other

reagents were of analytical grade and purchased from local vendors. Curcumin derivatives were synthesized using a previously described protocol.<sup>26</sup>

**UV–Visible Absorption Spectra of Curcumin.** Absorbance readings were taken from 250 to 550 nm using a Shimadzu (UV–vis) spectrophotometer. Degradation of curcumin was recorded, and UV–vis absorption spectra were collected at time 0, 5, 10, and 20 min. A stock solution of 10 mM curcumin was prepared in dimethyl sulfoxide (DMSO), and an appropriate volume of the curcumin solution was added to 50 mM phosphate buffer (pH 7.4) to achieve a final concentration of 10  $\mu\text{M}$ . A time-dependent degradation profile of curcumin was also measured in 50 mM 1,4-piperazinediethanesulfonic acid (PIPES) buffer at pH 7.4.

**Enhanced Curcumin Fluorescence upon Actin Binding.** Enhancement of the fluorescence of curcumin and its derivatives in the presence of actin was monitored using a Hitachi F-7000 fluorescence spectrophotometer at 25 °C. The experiment was carried out using a 0.5 cm path length quartz cuvette. Both the excitation and emission band passes were 5 nm. A different set of solutions were prepared in 50 mM PIPES containing 5  $\mu\text{M}$  actin in each along with 20  $\mu\text{M}$  curcumin and its derivatives, respectively. Each solution was incubated at 37 °C for 15 min. Subsequently, fluorescence emissions were recorded from 350 to 650 nm exciting the complexes at the absorption maxima of the respective ligands.

**Actin Polymerization Assay.** Lyophilized powder of pyrene-labeled rabbit muscle actin was reconstituted in general actin buffer [5 mM Tris-HCl (pH 8.0), 0.2 mM  $\text{CaCl}_2$ ] and polymerized at 25 °C in the presence of 50 mM KCl, 2 mM  $\text{MgCl}_2$ , and 1 mM ATP.<sup>27</sup> Enhancement of fluorescence was recorded on a fluorescence spectrophotometer connected to a constant temperature circulating water bath accurate to  $25 \pm 0.2$  °C, where excitation and emission wavelengths were kept at 350 and 407 nm, respectively. The experiment was carried out in a 0.5 cm path length quartz cuvette. The actin polymerization assay was performed in the presence of curcumin and its analogues using different concentrations for each compound.  $\text{IC}_{50}$  values were calculated by the concentration of compound that caused 50% inhibition of polymer mass.

**Isothermal Titration Calorimetry (ITC).** ITC measurements were taken on a VP-ITC microcalorimeter from MicroCal, Inc. (Northampton, MA, USA). Actin (20  $\mu\text{M}$ ) was dialyzed extensively against general actin buffer supplemented with 0.2 mM ATP, and the ligand (200  $\mu\text{M}$ ) was dissolved in the last dialyzant. A typical titration involved 13 injections of ligand (18  $\mu\text{L}$  aliquots/shot) at 3 min intervals into the actin-containing sample cell (volume of 1.4359 mL). The titration cell was kept at 25 °C and stirred continuously at 310 rpm. The heat of dilution of the ligand in the buffer alone was subtracted from the titration data. Data acquisition and analysis were performed using Microcal Origin 5.0 to determine the binding stoichiometry ( $N$ ) and other thermodynamic parameters of the reaction. The “One Set of Sites” binding model, provided with the software, was used. Enthalpy changes ( $\Delta H$ ) and affinity constants ( $K_a$ ) were known after the curve fitting. The changes in free energy ( $\Delta G$ ) and entropy ( $\Delta S$ ) were calculated using the equations

$$\Delta G = \Delta G^\circ + RT \ln K_a \quad (1)$$

$$\Delta G = \Delta H - T\Delta S \quad (2)$$

**Binding Measurements Using the Fluorescence Method.** We determined the affinity constant and stoichiometry for curcumin and its derivatives with actin by conventional Scatchard analysis<sup>28</sup> using the equation

$$\frac{r}{[L_{\text{free}}]} = nK_a - rK_a \quad (3)$$

Here,  $r$  is the number of moles of drug bound per mole of actin,  $[L_{\text{free}}]$  is the free drug concentration,  $K_a$  is the affinity constant, and  $n$  is the number of drug binding sites on actin.

We performed a reverse titration using the drug at 15  $\mu\text{M}$  with an increasing concentration of actin, and a standard curve was obtained when  $1/\text{fluorescence}$  was plotted against  $1/[\text{actin}]$ . From this curve, the fluorescence intensity corresponding to the 15  $\mu\text{M}$  ligand–actin complex was determined. To generate the binding isotherm, ligand (2–16  $\mu\text{M}$ ) was added to 15  $\mu\text{M}$  actin and each sample was incubated at 37 °C for 5 min. The actin–drug complexes were excited at the absorption maxima of the ligand. Hence, excitation wavelengths for curcumin, compound 2, compound 3, and compound 5 were kept at 427, 333, 327, and 413 nm, respectively. The amount of bound drug was determined by measuring the fluorescence at the corresponding wavelength of the respective emission maximum for each ligand. Because the bound drug concentration was known from the standard curve, the free drug concentration was calculated from the total drug concentration. We plotted  $r/[L_{\text{free}}]$  against  $r$ , and the affinity constant of the drug was calculated from the slope of the plot. All fluorescence measurements were carried out in a 0.5 cm path length quartz cuvette. Fluorescence values were corrected for the inner filter effect using the Lakowicz equation<sup>29</sup>

$$F_{\text{corrected}} = F_{\text{observed}} \left[ \text{antilog} \left( \frac{A_{\text{ex}} + A_{\text{em}}}{2} \right) \right] \quad (4)$$

where  $A_{\text{ex}}$  and  $A_{\text{em}}$  are the absorbance at the excitation and emission wavelengths, respectively.

**Cell Culture and Maintenance.** Human lung epithelium adenocarcinoma cells (A549) and human cervical cancer cells (HeLa) were cultured at 37 °C in a humidified atmosphere containing 5%  $\text{CO}_2$ . The cells were maintained in DMEM medium supplemented with 1 mM L-glutamine, 10% fetal bovine serum, 50  $\mu\text{g}/\text{mL}$  penicillin, 50  $\mu\text{g}/\text{mL}$  streptomycin, 2.5  $\mu\text{g}/\text{mL}$  amphotericin B, and nonessential amino acids. Cells were grown in tissue culture flasks until they were 80% confluent, at which point they were trypsinized and split.

**Immunofluorescence Assay of the A549 Cell Line.** A549 cells, grown in 6 well plates at ~60% confluency, were treated with latrunculin B (1 and 2  $\mu\text{M}$ ) and curcumin and its derivatives (20, 30, and 40  $\mu\text{M}$ ) for 24 h. Cells were washed twice with PBS to remove the chemicals and fixed through treatment with 3.7% formaldehyde solution for 20 min. The fixing solution was removed by repeated washes with PBS followed by treating the cells with 0.1% Triton X-100 for enhanced membrane permeabilization. The detergent from the wells was removed by repeated washes with PBS. Cells were then treated with blocking solution containing 3% BSA followed by incubation with 50  $\mu\text{g}/\text{mL}$  phalloidin conjugated with rhodamine solution and DAPI (1  $\mu\text{g}/\text{mL}$ ) for 1 h in the dark. The staining agents were washed out with PBS, viewed, and documented using a Zeiss confocal microscope (LSM 510 Meta).

**Docking and Simulation.** The structure used for actin was from rabbit skeletal muscle bound to lactrunculin A (PDB entry 1IJJ at 2.85 Å).<sup>30</sup> Chain A was considered for our studies. Missing residues (Met1–Glu4, Val43–Gln49, and Phe375) were modeled using Modeler.<sup>31</sup> The final modeled structure was subjected to docking with curcumin. AutoDock4<sup>32</sup> was first employed to generate the docked structures and then to determine the structures with the optimum number of hydrogen bonds (validated by HBPLUS<sup>33</sup>) and interactions in the simulations for 20 ns in explicit water at 300 K. All simulations and equilibration were performed using the sander module of the AMBER 10.0 software package.<sup>34</sup> The protein was solvated using a TIP3P box with the ff99SB force field parameters. The molecules were minimized using steepest descent for 500 cycles followed by the conjugate gradient method for 20000 cycles prior to the dynamics run. The system was heated to 300 K within 40 ps and equilibrated following minimization. Bonds involving hydrogen were constrained with the help of the SHAKE algorithm. The production run was carried out for 10 ns employing constant-pressure periodic boundary conditions. A nonbonded cutoff distance was set to 12 Å, and a 2 fs integration time step was used. The coordinates were saved after every 2 ps. Analyses of the trajectories were performed using the ptraj module of AMBER. To provide insight into the energetics of ligand binding, the simulation trajectories of the docked complex after 10 ns of simulation in explicit water were used to compute the binding energies of the small molecules by employing molecular mechanics generalized Born surface area (MM-GBSA) and Poisson–Boltzmann surface area (MM-PBSA) approaches.<sup>35</sup> For these, the last 5 ns of data were taken from the trajectory, and the interaction energies were calculated using scripts provided in the AMBER 10 package.<sup>36</sup> Generally, the free energy of receptor–ligand binding ( $\Delta G_{\text{binding,solvated}}$ ) is calculated by taking the difference between the free energies of the receptor–ligand complex ( $\Delta G_{\text{complex,solvated}}$ ) and the unbound receptor ( $\Delta G_{\text{receptor,solvated}}$ ) and ligand ( $\Delta G_{\text{ligand,solvated}}$ ) (eq 5).

$$\Delta G_{\text{binding,solvated}} = \Delta G_{\text{complex,solvated}} - [\Delta G_{\text{receptor,solvated}} + \Delta G_{\text{ligand,solvated}}] \quad (5)$$

Here,  $\Delta G_{\text{solvated}}$  is calculated by either solving for the linearized Poisson–Boltzmann or generalized Born equation for each of the three states ( $\Delta G_{\text{polar}}$ ) or adding an empirical term for hydrophobic contributions ( $\Delta G_{\text{nonpolar}}$ ). Solvent accessible surface area is used to calculate the hydrophobic contribution, and the entropic contribution is omitted for simplicity.

## RESULTS

Curcumin (1,7-bis(4-hydroxy-3-methoxyphenol)-1,6-hepta-diene-3,5-dione) is a palindromic molecule that contains two ferulic acid residues joined by a methylene bridge. Despite its wide range of medicinal properties, it is a very unstable molecule in aqueous solution at physiological pH.<sup>37,38</sup> Curcumin displays a UV–visible absorption spectrum containing an intense peak at 427 nm with a shoulder around 350 nm (Figure 1). Degradation of curcumin can be monitored easily from the change in its absorption profile over time in phosphate buffer at pH 7.4 (Figure 1A). It has been found that the intensity of the curcumin spectra decreases significantly over time. This extensive rate of degradation depends not only on the pH of the solution but also on the constituents of the



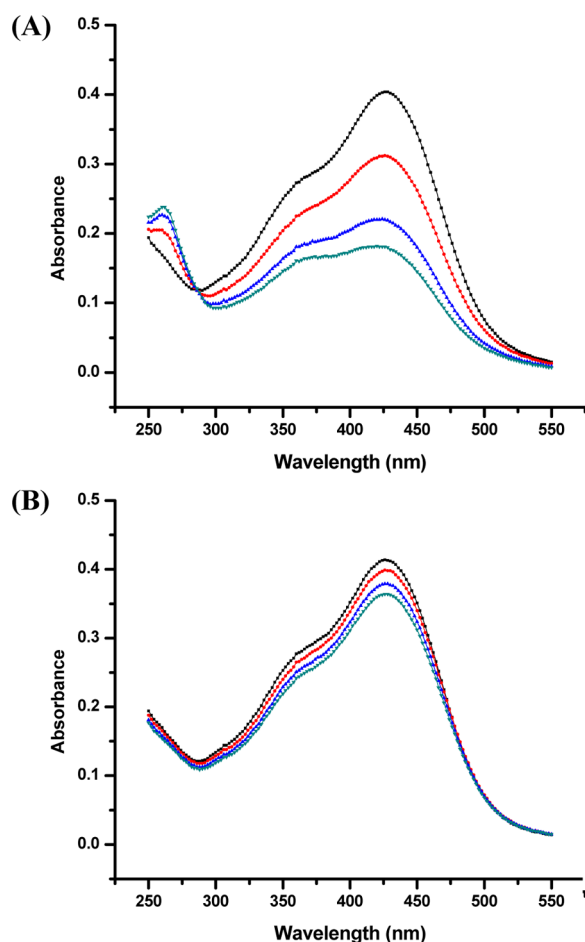


**Figure 1.** UV–visible absorption spectra of curcumin (10  $\mu$ M) in 50 mM (A) phosphate buffer (pH 7.4) and (B) PIPES buffer (pH 7.4). Measurements were taken at 0 (black squares), 5 (red circles), 10 (blue triangles), and 20 (green inverted triangles) min.

buffer. We found that the rate of curcumin degradation at pH 7.4 in Good's buffers such as PIPES is lower than that in phosphate buffer at the same pH (Figure 1B). Curcumin stability is a generalized problem when trying to use it for biophysical assays.

**Enhanced Curcumin Fluorescence upon Binding to Actin.** Curcumin is weakly fluorescent in aqueous solution<sup>26</sup> but shows intense fluorescence in the presence of actin with a large blue shift in the spectra from 520 to 500 nm (Figures S1 in the Supporting Information). Generally, hydrophobic molecules show this type of spectral characteristic when there is a change in the local environment of the molecule; binding to the hydrophobic pocket of protein leads to enhanced fluorescence with a blue shift in the emission maximum. This extent of fluorescence enhancement has also been found for curcumin in the presence of polymeric actin, indicating that curcumin can bind to both monomeric and polymeric actin (data not shown). We next verified the binding capacities of all of the curcumin derivatives (Table 1) to actin through fluorescence tests (Figure 2). Substitution in the diketone group of curcumin with an oxazole or pyrazole ring (in compounds 2 and 3, respectively) produces structural modifications that hinder extended conjugation, resulting in a blue shift in the absorption maximum relative to that of curcumin.<sup>26</sup> We therefore excited the compound 2 and 3 complexes with actin at their characteristic wavelength maxima

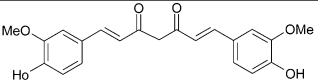
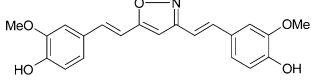
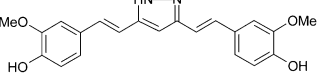
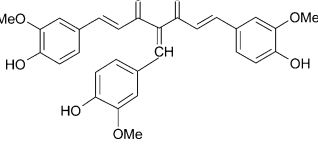
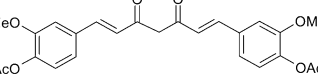
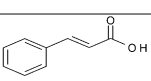
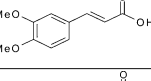
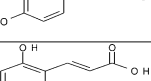
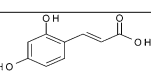
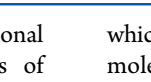
of 333 and 327 nm, respectively. Only a few of the derivatives (compounds 2, 3, and 5) displayed similar fluorescence enhancement in the presence of actin, indicating binding; the rest showed no change in fluorescence.

**Effect of Curcumin on Actin Polymerization.** Following the results from the fluorescence experiments, we wanted to determine if the binding of curcumin to actin affects G- and F-actin equilibrium (an important diagnostic marker of the actin system<sup>4</sup>). We tested actin polymerization in the presence of curcumin using 1 mM ATP. In vitro, curcumin shows progressive concentration-dependent inhibition of actin self-assembly with an  $IC_{50}$  of 16  $\mu$ M (Figure 3). The effect of substitution on the curcumin structure was evaluated by performing the polymerization assay with the curcumin derivatives; the  $IC_{50}$  values are shown in Table 1. Compound 2 (oxazole-curcumin) retains actin polymerization inhibitory activity similar to that of curcumin, whereas the inhibitory effect of compound 3 (pyrazole-curcumin) is reduced significantly as reflected by its higher  $IC_{50}$  value. Interestingly, benzylidene substitution at the C-4 position in compound 4 causes its inhibition of polymerization to increase significantly (4 times higher than that of curcumin). This benzylidene derivative was also the strongest inhibitor of tubulin polymerization into microtubules.<sup>26</sup> Acetylation of curcumin (compound 5) does not change the inhibitory effect significantly. Half compounds 6–10, which have a half equivalent structure of curcumin, failed to show inhibitory activity, indicating that their chemical structures do not possess the conditions necessary for actin binding and thus for inhibition of polymerization.

**Determination of Thermodynamic Parameters and Binding Constants.** Here, we determined the thermodynamic parameters for changes in Gibbs free energy ( $\Delta G$ ), enthalpy ( $\Delta H$ ), and entropy ( $\Delta S$ ) along with the number of binding sites ( $N$ ) and affinity constant ( $K_a$ ). These parameters provide useful information for understanding the fundamental forces involved in protein–ligand interactions. We also determined binding enthalpy as a function of temperature that yields changes in heat capacity ( $\Delta C_p$ ). However, we were unable to perform ITC experiments because of the low solubility and instability of curcumin in aqueous solution at pH  $\geq 7$ . We have shown previously that curcumin is very unstable at physiological pH, especially in the presence of reducing agents like alkaline pH and others; however, stability is attained after substituting the 1,3-diketone group (midsection) for an oxazole or pyrazole moiety.<sup>39</sup> As such, compound 2 was chosen for titration with actin.

Figure 4 shows the raw data of a calorimetric experiment for the titration of actin with compound 2. It is evident that the binding reaction is characterized by a significant amount of heat change with a stoichiometry ratio of 1.13 (Table 2). The binding affinity constant was found to be  $7.20 \times 10^5 \text{ M}^{-1}$  at 25 °C. Actin binding to compound 2 is driven by simultaneous participation of favorable van der Waals (negative  $\Delta H$ ) and hydrophobic interactions (positive  $\Delta S$ ). The total entropy change of drug–protein interactions is composed of three components, namely, solvation entropy ( $\Delta S_{\text{solv}}$ ), conformational entropy ( $\Delta S_{\text{conf}}$ ), and rotational–translational entropy ( $\Delta S_{\text{r/t}}$ ), which were calculated using a previously published procedure.<sup>26</sup> The binding reaction is associated with a favorable contribution of solvation entropy that overcomes the unfavorable contribution of conformational entropy, as reflected by their respective values (Table 2). The unfavorableness associated with the change in conformational entropy

Table 1. Chemical Structures and Half-Maximum Polymerization Inhibition Values of Various Curcumin Analogues

Name of the ligand	Structure	Half-maximum polymerization inhibition value ( $\mu\text{M}$ )
Curcumin		16
Compound2		23
Compound3		50
Compound4		4.5
Compound5		26
Compound6		---
Compound7		---
Compound8		---
Compound9		---
Compound10		---

in protein–ligand binding (negative change in conformational entropy) is due to the loss of configurational degrees of freedom for both the drug and the protein molecules. The unfavorable effect can be reduced by using a conformationally rigid drug molecule.<sup>40</sup> For actin–compound 2 binding, the change in conformational entropy is  $-6.38 \text{ cal K}^{-1} \text{ mol}^{-1}$ . The small change in conformational entropy is attributed to the rather rigid nature of compound 2. It is apparent from this discussion that the unfavorable (negative) conformational entropy change is overcompensated by a large favorable (positive) solvent contribution that leads to an overall gain in entropy. The thermodynamic parameters  $\Delta H$  and  $\Delta S$  were determined over a range of temperatures from 25 to 35 °C, and the heat capacity change at constant pressure ( $\Delta C_p$ ) was determined using the Kirchoff equation  $\Delta C_p = d\Delta H/dT$  (Table 3). The  $\Delta C_p$  is estimated to be  $-277 \text{ cal K}^{-1} \text{ mol}^{-1}$ ; the negative  $\Delta C_p$  value indicates the involvement of hydrophobic interactions between the protein and drug. For interactions during the formation of protein–protein and protein–ligand complexes,  $\Delta C_p$  is usually negative because these types of interactions are associated with burial of surface molecules at the binding interface and thus removal of interfacial water. A similar mechanism is most likely involved in the reaction between the highly hydrophobic ligand curcumin and actin,

which would result in the removal of a large number of solvent molecules from the actin–curcumin interfacial surface.

On the basis of the low solubility and instability of aqueous curcumin, ITC experiments could not be performed to determine the binding and thermodynamic parameters for curcumin and some of its derivatives. Therefore, we determined the affinity constants and the stoichiometry of binding for these compounds using Scatchard analysis.<sup>28</sup> Details of the analysis have been provided in the Materials and Methods. Results given in Figure S2 in the Supporting Information indicate that the stoichiometry of the curcumin–actin interaction is  $\sim 1:1$ . The affinity constant ( $K_a$ ) of the curcumin–actin interaction is  $(2.45 \pm 0.01) \times 10^5 \text{ M}^{-1}$  at 37 °C (Table 4). The association constant values for other curcumin derivatives were determined in a similar manner (Table 4) and correlated well with their  $\text{IC}_{50}$  values, which correspond to 50% inhibition of actin polymerization. The decrease in  $K_a$  (and concomitant increase in  $\text{IC}_{50}$ ) is in the order curcumin  $\rightarrow$  compound 2  $\rightarrow$  compound 5  $\rightarrow$  compound 3. Our results suggest that the dicarbonyl moiety of curcumin is involved in its interaction with actin. Also, the substitutions of pyrazole and oxazole in place of the dicarbonyl moiety of curcumin do not contribute to identical structural changes. Our results also suggest that the phenolic hydroxyl group of curcumin is involved in the interaction with

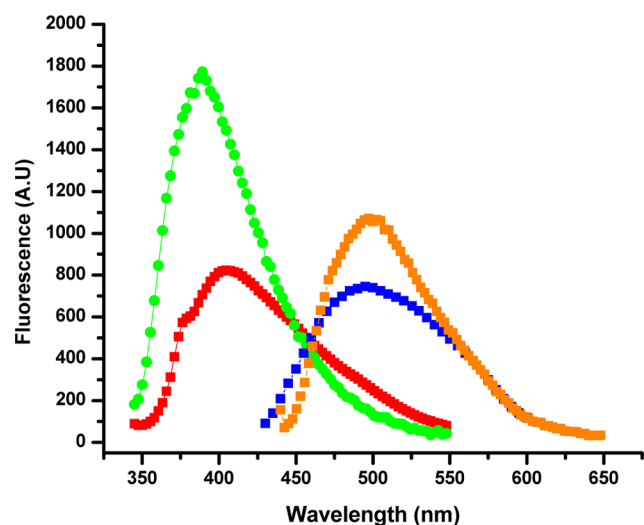


**Figure 2.** Fluorescence spectra of different curcumin analogues in the presence of actin. The complexes were prepared using 5  $\mu\text{M}$  actin and 20  $\mu\text{M}$  ligand in 5 mM PIPES buffer (pH 7.4) at 37  $^{\circ}\text{C}$ , and then their fluorescence responses were measured after exciting the ligands at their characteristic absorbance maxima of 427, 333, 327, and 413 nm for curcumin (orange squares), compound 2 (red squares), compound 3 (green circles), and compound 5 (blue squares), respectively.

actin. The benzylidine analogue of curcumin, compound 4, which is the most efficient in inhibiting the self-assembly does not fluoresce when bound to actin. Apart from these derivatives, the half analogues showed no interaction with actin which is also suggested from the polymerization assay.

**Immunofluorescence Assay.** The actin filament network is a vital cytoskeletal structure that contributes to the morphological features of a cell and participates in the dynamic regulation of cellular functions.<sup>1,4</sup> This actin cytoskeleton is reorganized during mitosis to form rounded cells with increased cortical rigidity but is re-established after mitosis to allow cells to regain their extended shape and attachment to the substratum.<sup>4</sup> The integrity of the organization of the actin network relative to the phases of mitosis clearly implies a functional role for actin in cell division. To observe the effects

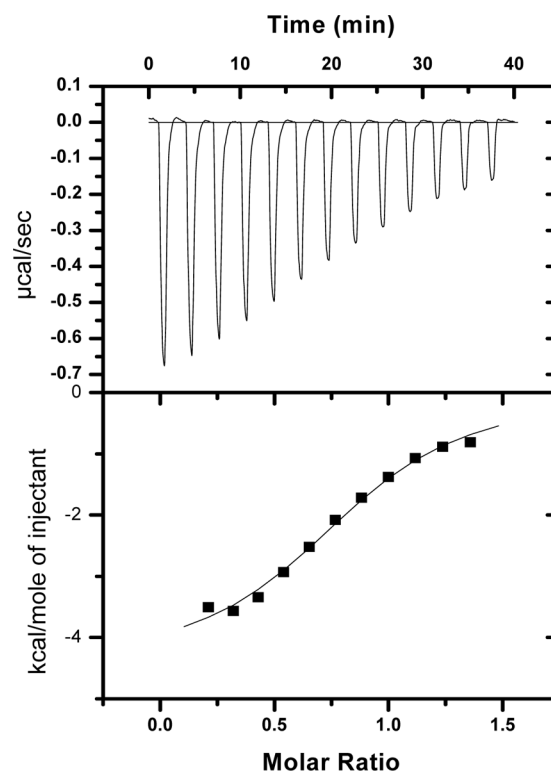


**Figure 4.** Calorimetric titration of compound 2 with actin. The upper panel shows raw data obtained from 13 injections (19  $\mu\text{L}$  each) of compound 2 (300  $\mu\text{M}$ ) into 30  $\mu\text{M}$  actin in 5 mM Tris buffer containing 0.2 mM  $\text{CaCl}_2$  at pH 8.0. The lower panel shows a nonlinear least-square fit of the incremental heat per mole of added ligand for titration in the upper panel as a function of molar ratio using Origin 5.0 software.

of curcumin on morphological changes of the actin network, we performed immunofluorescence assays. Human lung epithelial cells (A549) were chosen as control cells because they have abundant stress fibers that extend across the cytoplasm. We have found that A549 control cells treated with 0.5% DMSO have a well-organized F-actin network distributed both throughout the cell and at the periphery (Figure 5A). However,

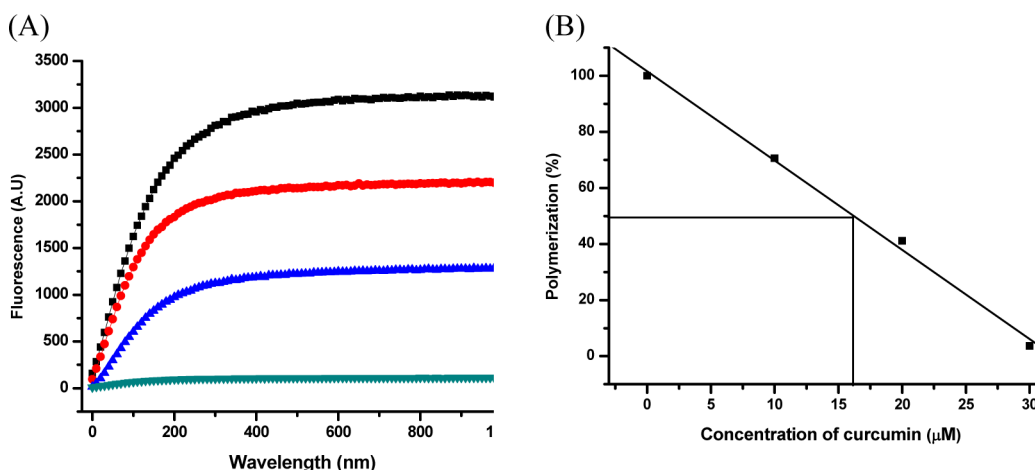


**Figure 3.** Actin polymerization assay. (A) Pyrene-labeled actin polymerization was performed in G-actin buffer (5 mM Tris-HCl, 0.2 mM  $\text{CaCl}_2$ , pH 8.0). The reaction was initiated with 1 mM ATP, 50 mM KCl, and 2 mM  $\text{MgCl}_2$ . The assay was performed in the presence of 0 (black squares), 10 (red circles), 20 (blue triangles), 30  $\mu\text{M}$  (green inverted triangles) curcumin. Excitation and emission wavelengths were set at 350 and 407 nm, respectively. (B) Plot of the percentage of polymerization vs the concentration of curcumin used.

**Table 2. Thermodynamics of Actin–Compound 2 Binding at 30 °C**

thermodynamic parameter	value
<i>N</i> (drug–protein stoichiometry)	1.13
<i>K<sub>a</sub></i> (binding constant, <i>M</i> <sup>−1</sup> )	$7.20 \times 10^5$
$\Delta H$ (binding enthalpy, cal mol <sup>−1</sup> )	−2548
$\Delta S_{\text{tot}}$ (entropy change, cal K <sup>−1</sup> mol <sup>−1</sup> )	18.5
$\Delta S_{\text{solv}}$ (solvation entropy change, cal K <sup>−1</sup> mol <sup>−1</sup> )	32.88
$\Delta S_{\text{conf}}$ (conformational entropy change, cal K <sup>−1</sup> mol <sup>−1</sup> )	−6.38
$\Delta S_{\text{r/t}}$ (rotational–translational entropy change, cal K <sup>−1</sup> mol <sup>−1</sup> )	−8
$\Delta G$ (free energy change, kcal mol <sup>−1</sup> )	−8.15

**Table 3. Heat Capacity Changes of Actin–Compound 2 Interactions**

temperature (K)	$\Delta H$ (cal mol <sup>−1</sup> )	$\Delta S$ (cal K <sup>−1</sup> mol <sup>−1</sup> )	$\Delta C_p$ (cal K <sup>−1</sup> mol <sup>−1</sup> )
298	−1660	23	−277
303	−2548	18.5	
308	−4431	9.54	

**Table 4. Association Constants of Different Curcumin Analogues with Actin Obtained Using a Scatchard Plot**

ligand name	affinity constant ( <i>K<sub>a</sub></i> , <i>M</i> <sup>−1</sup> )
curcumin	$(2.45 \pm 0.01) \times 10^5$
compound 2	$(2.18 \pm 0.02) \times 10^5$
compound 3	$(8.29 \pm 0.001) \times 10^4$
compound 5	$(1.93 \pm 0.019) \times 10^5$

treatment of the cells with a concentration of curcumin ranging from 20 to 40  $\mu\text{M}$  caused disruption of the actin microfilament network (Figure 5D–F). In addition, actin aggregates have been found to localize under the plasma membrane. Some cells had brightly fluorescent actin fibers localized at only the outside edge of the cell. Some cells had an overall diffuse, disorganized network rather than the evenly organized actin network found in control cells. Our results indicate that curcumin induces disorganization of the normal actin microfilament network in A549 cells. We compared this result with those of cells that were treated with latrunculin B (an actin network disrupting drug).<sup>30,41</sup> We found more diffuse F-actin staining and a reduced number of fibers throughout the cell after treatment with latrunculin B (Figure 5B,C). We have also performed the immunofluorescence assay with the stable and active analogue compound 2 and found a similar diffuse, disorganized actin network (Figure 5G–I).

**Binding Site Determination.** Our experimental results suggest that curcumin is an actin filament destabilizing compound that binds to actin and perturbs the dynamic equilibrium between actin and microfilament. Known actin inhibitors that block or destabilize actin filaments have been shown to do so by binding to two distinct regions of the actin monomer: (i) the ATP binding cleft and (ii) the barbed end (Figure S3 in the Supporting Information).<sup>42,43</sup> Actin filaments are known to have structural polarity with the actin subunits being aligned in such a way that one end of the molecule (the pointed end where the ATP binding cleft is located) interacts with the opposite end (the barbed end) of a neighboring monomer.

To gain a better understanding of the nature of curcumin binding, we have carried out docking studies separately using both the keto and enol forms. Docking results show that

various configurations of curcumin have a comparable binding energy at different sites of the actin structure and that many different conformations are suitable for maximizing hydrophobic contacts with the protein residues. Among these, the most favorable (i.e., lowest energy) binding was found at the barbed end of monomeric actin, which is very close to the binding site of cytochalasin-D (PDB entry 1EKS), a fungal toxin that interferes with the normal dynamics of the actin cytoskeleton by binding to the barbed end of actin filaments (Figure 6).<sup>44,45</sup> Docking results also exemplify the fact that curcumin binding is far removed from the ATP binding cleft of the actin monomer, which is where the latrunculin type of cytotoxins usually binds.<sup>30,41</sup> This observation is also supported by the fact that the emission maximum of curcumin complexed to actin is not altered in the presence of latrunculin B (data not shown), indicating that curcumin does not possess a binding site identical to that of latrunculin B. The lowest binding energy for the keto form of curcumin was  $-5.78 \text{ kcal mol}^{-1}$ , and that of the enol form was  $-4.22 \text{ kcal mol}^{-1}$ . This may be explained by the number of hydrogen bonds involved in binding. We found that three hydrogen bonds occur in the binding pocket (involving the Arg118 (NH<sub>2</sub>), Tyr145 (OH), and Cys376 (SG) residues) for the keto conformation of curcumin. Conversely, only a single hydrogen bond was found for the enol conformation (involving the Leu110 (NH) residue). Thus, the keto form provides a lower binding energy with a larger number of hydrogen bonds. In addition, curcumin also uses its aromatic rings to interact with hydrophobic residues located near its binding site. On the basis of these results, it can be concluded that the combination of hydrophobic interactions and extensive hydrogen bonding gives curcumin many favorable ways to bind to actin.

**Molecular Dynamics.** To better understand the inherent flexibility of the ligand and its interactions with binding site residues, we performed molecular dynamics simulations using both the actin–ATP structure and the complex formed between actin–ATP and the keto form of curcumin. From simulations of the unbound receptor (actin–ATP), we find that actin itself is very flexible, particularly in subdomain 2 (residues 36–71, especially in D-loop residues 40–49) and a loop in subdomain 4 (residues 197–207) (Figure 7, Movie SM1 in the Supporting Information). These observations are corroborated by the residue-wise root-mean-square fluctuation (RMSF) profile (Figure S4 in the Supporting Information). The D-loop is disordered in most crystal structures of actin, but it plays an important role in actin polymerization.<sup>46–48</sup> ATP has been shown to form hydrogen bonds mostly with Ser16 (subdomain 1) and Asp156 and Tyr308 (subdomain 3). Simulations reveal ATP drift toward subdomains 1 and 3 (the cofactor's center of mass changes by 3.1 Å), forming hydrogen bonds with residues Pro111 and Tyr171, respectively. The root-mean-square deviation (RMSD) values, which inform about gross structural changes to a protein over time, increase to 4.5 Å toward the end of the simulation (Figure S4 in the Supporting Information).

Simulation of the complex shows a shift of the ligand toward subdomain 3 within the first few nanoseconds (Figure 8, Movies SM2 and SM3 in the Supporting Information). Initial contact of the ligand with residues having aromatic and hydrophobic groups, including Pro111, Ile138, Val141, Tyr145, Ile177, and Leu348, is maintained throughout the time scale of the simulation. A few new interactions are formed, including with Thr150, Val165, Gly170, Tyr171, Ala172, Leu173, Pro174, and Phe354, at the end of the simulation. The binding site is



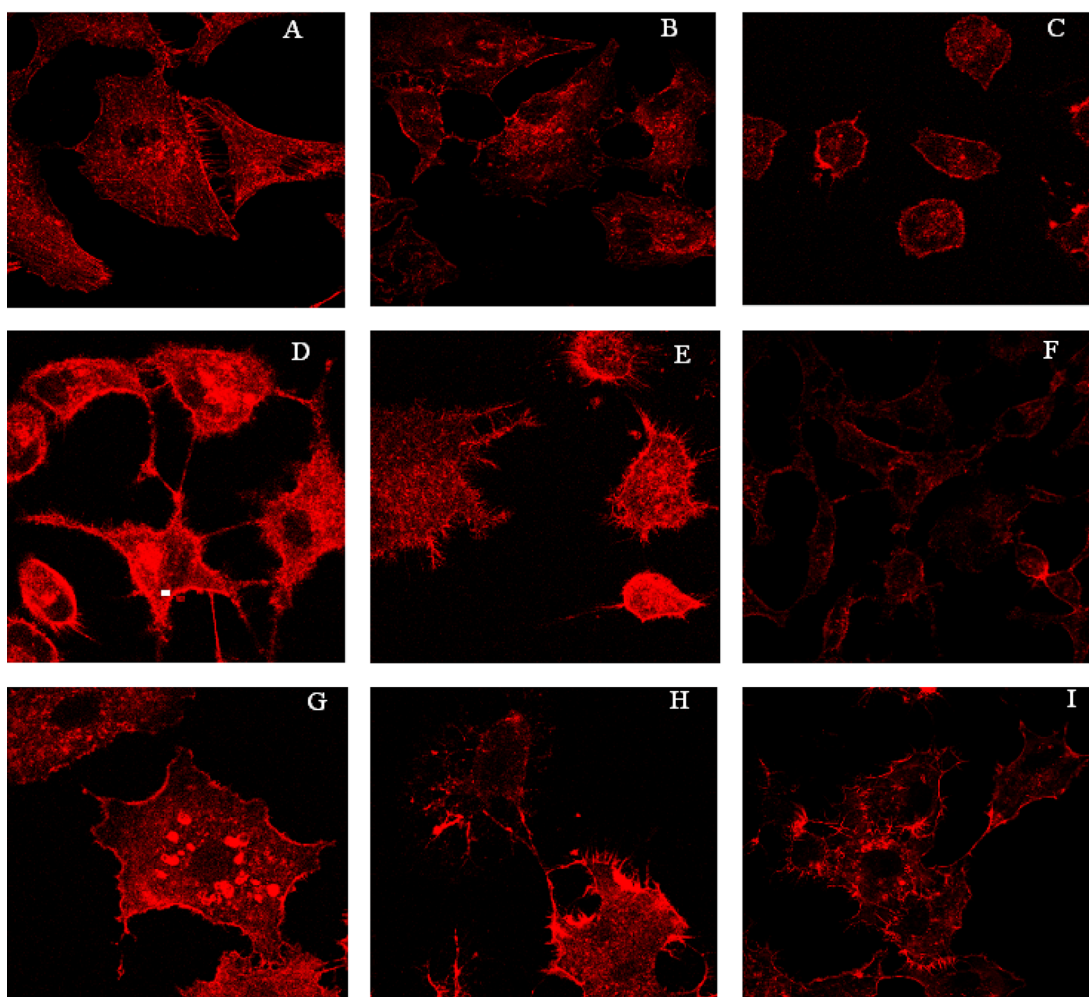


**Figure 5.** Disruption of the microfilament network in cultured A549 cells through drug treatment in an immunofluorescence assay. Microfilament images of untreated cells (A) and cells treated with 1 and 2  $\mu\text{M}$  latrunculin B (B and C, respectively); 20, 30, and 40  $\mu\text{M}$  curcumin (D–F, respectively); and 20, 30, and 40  $\mu\text{M}$  compound 2 (G–I, respectively) taken using a Zeiss confocal microscope. In each case, the DMSO concentration was maintained at 0.4%.

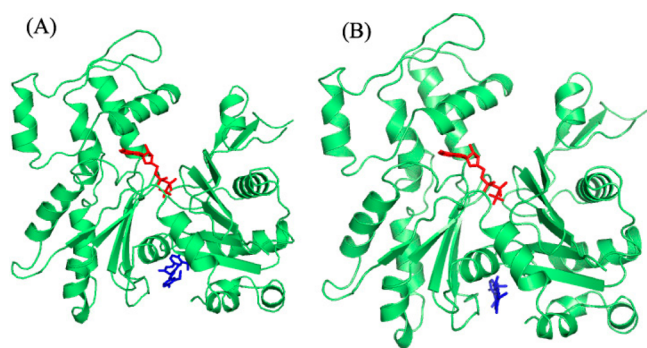


**Figure 6.** Molecular docking of actin (PDB entry 1IJJ at 2.85 Å) with the (A) keto and (B) enol forms of curcumin. Red sticks represent ATP, and blue sticks represent curcumin. Molecular docking was performed using AutoDock4 software (version 1.5.6).

more hydrophobic after 20 ns (the grand average of hydropathy (GRAVY) increases from 0.33 to 1.93, <http://www.gravy-calculator.de/index.php>). Overall structural deviations are reflected in the RMSD profile of the protein; the RMSD value increases to  $\sim 3$  Å in the first few picoseconds to reach a final value of 4.1 Å after 20 ns. The plot shows no such

difference between the unbound and complexed structure. A slight decrease of RMSD is observed in the bound structure, which indicates a marginal increase in overall rigidity imparted by binding of the ligand. The flexible regions of the protein are described by the RMSF plot, which shows a trend similar to that of the unbound structure, indicating no major change in the flexibility of the protein. We also find here that residues 42–52 (corresponding to the D-loop) have high values, which followed the region ranging from 200 to  $\sim 250$  (subdomain 4). These form a piece of the pointed end of actin that is associated with polymerization of the protein.<sup>46</sup> The ligand binds at the barbed end, affecting internal hydrogen bonding between residues of subdomains 1 and 3. In the uncomplexed protein, Tyr171 (subdomain 3) and Lys375/Cys376 (subdomain 1) form interdomain hydrogen bonds that are lost upon ligand binding. The hydrogen bonds between ATP and Pro111, as seen for the unbound protein, are also disrupted, and new contacts with curcumin are observed for the complex. Movement of ATP toward subdomains 1 and 3 is impeded when ligand binds (the molecule's center of mass changes by 2 Å), preventing interactions between the nucleotide and residues from subsequent regions. From the average  $\Delta G_{\text{binding}}$  calculated employing both MM-PBSA and MM-GBSA, we find ligand



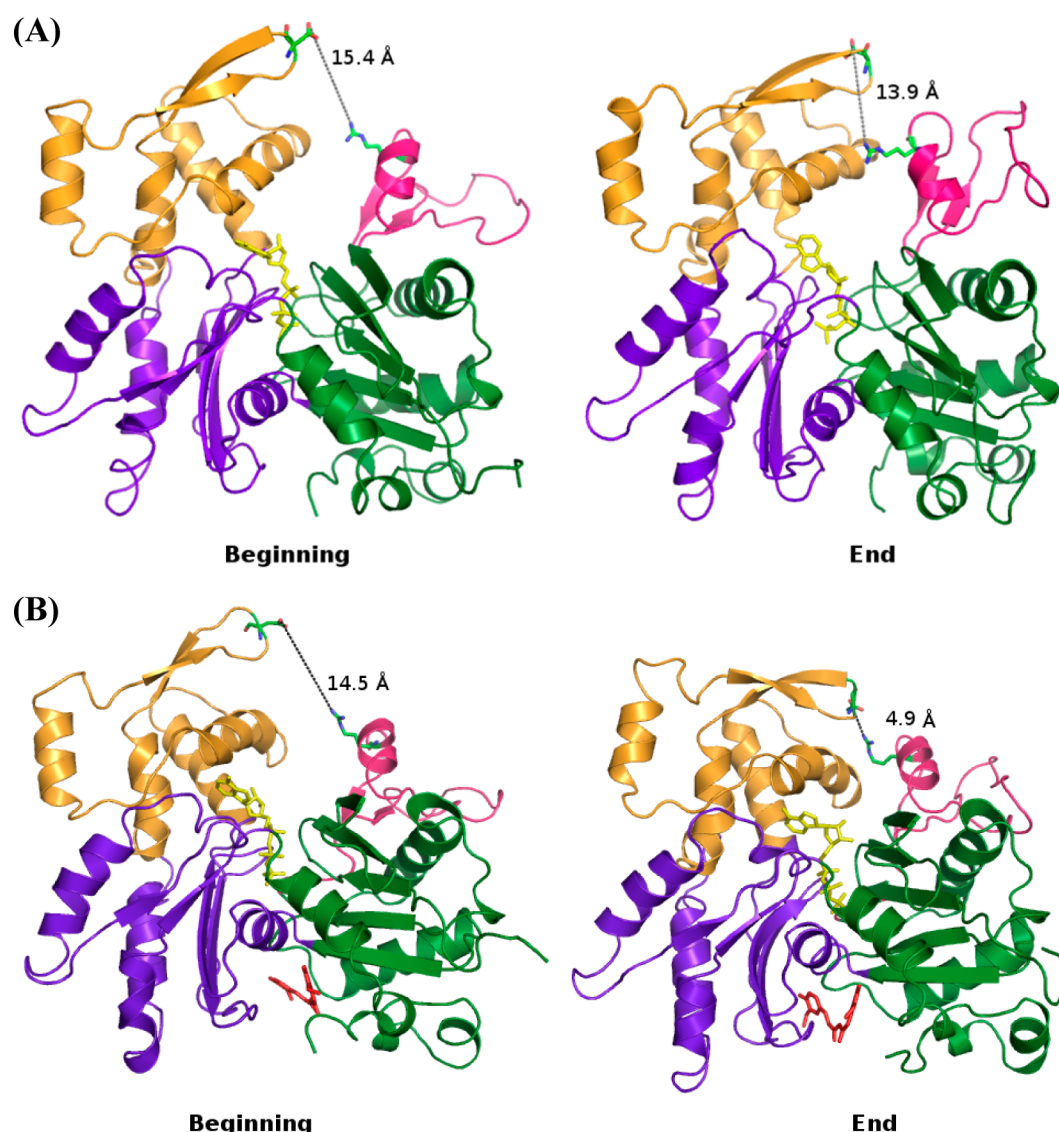


**Figure 7.** Representation of the structures at the beginning and end of the time period for (A) actin–ATP and (B) actin–ATP complexed with curcumin. The four subdomains of the protein are shown in different colors (subdomain 1: residues 1–35, 76–137, and 339–377; 2: residues 36–75; 3: residues 138–184 and 270–338; and 4: residues 185–269) along with ATP (yellow sticks) and curcumin (red sticks). Arg64 (subdomain 2) and Asp246 (subdomain 4) are represented by sticks colored by elements; the distances between them are indicated.

binding to be favorable as both the protein and ligand undergo considerable change during the simulation (Table 5).

We find that the subdomains constituting the pointed end of the structure (i.e., residues 36–72 (subdomain 2) and 185–269 (subdomain 4)) gradually come closer together (Movie SM2 in the Supporting Information). It is fascinating to find that even though the ligand binds at the barbed end its effect is reflected at the pointed end, which becomes constrained as subdomains 2 and 4 are brought into close proximity. A salt bridge is formed between Asp246 of subdomain 4 and Arg64 of subdomain 2 from ~2 to 11 ns; then, the two residues move apart, ultimately coming closer together again to form contacts at the end of the 20 ns simulation (Movie SM2 in the Supporting Information). This interaction alters the intermediate space between the two subdomains, making it narrow and more constrained (Figure 7). Toxins that block or destabilize actin filaments usually bind near the ATP binding cleft or at the barbed end. Here, we find an allosteric effect in which the binding of curcumin at the

barbed end is reflected as a change in the pointed end, which may cause filament disorganization.

## DISCUSSION

Curcumin, the active ingredient in turmeric (*C. longa*), has been utilized as medicine for a wide range of diseases, including cancer.<sup>18–20</sup> But the question of how it possesses such a vast array of medicinal properties remains unresolved. Extensive research over the past 30 years indicates that this molecule has numerous targets in a cell and that a number of different mechanisms may be at work to exhibit its diverse properties.<sup>18,21,22</sup> It is unique in recognizing and binding to many different types of proteins, including enzymes,<sup>49</sup> protein kinases,<sup>50</sup> protein reductases,<sup>51</sup> carrier proteins,<sup>52</sup> inflammatory molecules,<sup>53</sup> DNA,<sup>54</sup> RNA,<sup>55</sup> and so forth. In most of these cases, the precise mode of curcumin binding has not been elucidated. On the basis of observations of Holy<sup>25</sup> and Chen et al.,<sup>24</sup> the microfilament network of the cell cytoskeleton appears to be destabilized in the presence of curcumin. This similar

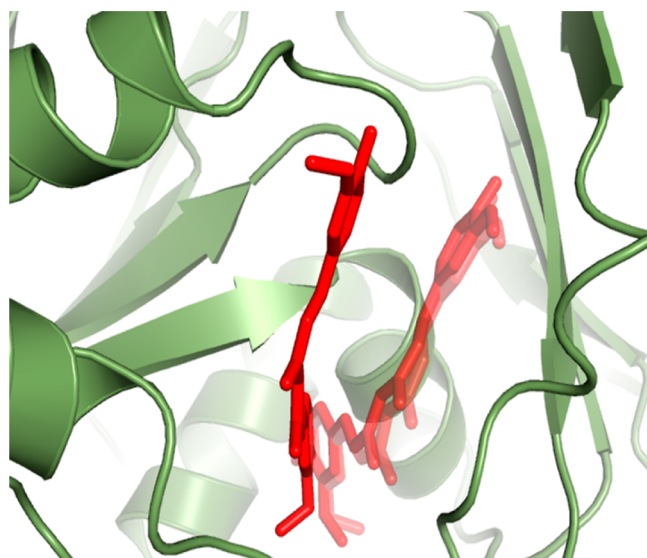


**Figure 8.** Amplification of the curcumin binding site showing the shift of the ligand position. The receptor is represented by the green cartoon and the ligand by red sticks with an increasing level of transparency depicting the trail of motion from its initial point.

observation from different groups led us to investigate whether curcumin could bind to actin and inhibit microfilament formation, and that if it could, to determine the mechanism of action by which it could inhibit actin polymerization. In this study, we have examined actin–curcumin interactions in detail with purified actin, and we have found that curcumin binds to actin (affinity constant  $K_a = (2.45 \pm 0.01) \times 10^5 \text{ M}^{-1}$  (Table 4)) and inhibits its polymer formation into microfilaments ( $\text{IC}_{50} \cong 16 \mu\text{M}$ ) (Table 1). The results establish that “actin–microfilament dynamics” is another target of curcumin. It is remarkable that curcumin also inhibits tubulin polymerization with a dissociation constant of  $20 \mu\text{M}$  (previously reported by our lab),<sup>26</sup> indicating that it has a similar affinity for both the cytoskeleton proteins tubulin and actin. However, another group reported that the dissociation constant value for tubulin–curcumin interaction was  $2.4 \mu\text{M}$ , which could be due to differences in solution conditions, the polymer inducer used during protein purification, or the stability of curcumin itself.<sup>56</sup>

We synthesized a large number of curcumin analogues and tested each of them to determine their efficacy for inhibiting actin self-assembly. Our study with these various analogues shows that curcumin acts as a bifunctional ligand in the self-assembly of both tubulin<sup>26</sup> and actin; diketone-substituted analogues and acetylation of terminal phenolic groups are less effective, whereas a benzylidene derivative is more potent, than curcumin at inhibiting actin self-assembly. It thus appears that particularities of the structure of curcumin, such as the two aromatic end groups and a suitable linker length between them, are essential criteria for the manifestation of its optimal inhibitory activity.

Thermodynamic parameters of binding were determined for the stable curcumin analogue compound 2 across a range of temperatures. The binding is enthalpy driven with a large negative  $\Delta C_p$  (Table 3), indicating the involvement of hydrophobic interactions between the ligand and protein. The favorable change in  $\Delta H$  signifies that van der Waals interactions and hydrogen bonding also play a prominent role in the formation of the drug–actin complex. Additionally, we observed the formation of a salt bridge between two subdomains of actin that was induced by narrowing of the inter-region space by curcumin binding (Figure 7). Molecular dynamics studies indicated that binding of curcumin to actin produced an allosteric effect, as ligand binding at the barbed end makes the intersubdomain space in the pointed end narrower, adversely affecting interactions between adjacent actin monomers during polymerization. Because curcumin does not possess any structural resemblance to other known actin inhibitors, this mechanism of inhibition is most likely unique.

Curcumin targets a variety of cellular proteins regardless of their sequence, structure, function, and so forth. It has also been shown to possess the exceptional property of inhibiting protein polymerization/aggregation.<sup>26,56–59</sup> Thus, understanding how curcumin exhibits a similar effect on two dynamic protein systems, namely microtubules and microfilaments, is paramount. A few particular characteristics of the molecule may be pertinent. For both systems, the binding is thermodynamically favorable with a negative  $\Delta H$  and positive  $\Delta S$ . The polar nature of curcumin may be due to the presence of two phenolic hydroxyl groups, two methoxy groups, and two ketone moieties situated in the middle. On the other hand, the hydrophobic character of curcumin is due to the presence of two aromatic phenol rings. In general, during protein polymerization or aggregation, the exposed hydrophobic surface of one protein comes close to the hydrophobic surface of a neighboring protein molecule, making energetically favorable contacts. It is possible that curcumin competes with the protein–protein hydrophobic interaction through its hydrophobic aromatic moieties to prevent polymerization/aggregation. Furthermore, flexibility in the curcumin structure (due to the presence of a flexible, conjugated 7-carbon chain) is an advantageous feature augmenting its binding capacity.<sup>58</sup> It may thus adopt various configurations thereby allowing it to maximize hydrophobic contacts with the protein to which it binds. This flexibility may help to make it functional across a large variety of proteins, enzymes, peptides, DNA, and so forth. Moreover, the involvement of both polar and nonpolar groups beautifully choreographed in the curcumin structure makes it amenable to binding a large variety of divergent proteins.

## ■ ASSOCIATED CONTENT

### § Supporting Information

Additional experimental details, fluorescence emission spectra of curcumin and its derivatives in the absence and presence of actin, fluorescence titration of actin with curcumin, representation of actin and its different regions, RMSD and RMSF

**Table 5. Estimation of Protein–Ligand Binding Energy in the Actin–Curcumin Complex Using the MM-GBSA and MM-PBSA Approaches**

structure	MM-GBSA average $\Delta G_{\text{binding}}$ (kcal mol <sup>−1</sup> )	MM-PBSA average $\Delta G_{\text{binding}}$ (kcal mol <sup>−1</sup> )	RMSD <sub>ligand</sub> after 20 ns (Å)	RMSD <sub>protein</sub> after 20 ns (Å)
actin–curcumin	$-32.2 \pm 9.1$	$-38.6 \pm 9.1$	1.1	4.1 <sup>a</sup>

<sup>a</sup>A value of 4.5 Å was found when actin alone was subjected to the simulation.

profiles, dynamics of actin–ATP in the absence and presence of curcumin (SM1 and SM2, respectively), and an enhanced view of the curcumin binding site (SM3). This material is available free of charge via the Internet at <http://pubs.acs.org>.

## AUTHOR INFORMATION

### Corresponding Authors

\*E-mail: [surolia@mbu.iisc.ernet.in](mailto:surolia@mbu.iisc.ernet.in). Tel: 91-80-2293-2714. Fax: 91-80-2360-0535

\*E-mail: [bablu@mail.jcbose.ac.in](mailto:bablu@mail.jcbose.ac.in). Fax: 91-332-2334-3886. Tel: 91-332-2337-9544.

### Funding

This work was supported by the Raja Ramanna Fellowship from the Department of Atomic Energy to B.B. P.C. and A.S. are recipients of JC Bose National Fellowships from the Department of Science and Technology (DST). A.S. holds a Bhatnagar Fellowship from the Council of Scientific and Industrial Research (CSIR) in India. M.P. acknowledges a grant from the DST and Department of Biotechnology (DBT). G.D. acknowledges a fellowship from CSIR.

### Notes

The authors declare no competing financial interest.

## ACKNOWLEDGMENTS

We thank Suman Mukherjee, a guest worker from the Haldia Institute of Technology, for his suggestions.

## ABBREVIATIONS

SDS–PAGE, sodium dodecyl sulfate–polyacrylamide gel electrophoresis; DMEM, Dulbecco's modified Eagle's medium; PBS, phosphate buffered saline; DTT, dithiothreitol; BSA, bovine serum albumin; DAPI, 4',6-diamidino-2-phenylindole; MTT, 3-(4,5-dimethylthiazol-2-yl)-2,5-diphenyltetrazolium bromide; PDB, Protein Data Bank; D-Loop, Residues 40–49 In Subdomain 2 Of Actin That Comprise Part Of The Dnase I Binding Site; Lncap, Human Prostate adenocarcinoma cell line; PC-3, human prostate cancer cell line; RMSF, root-mean-square fluctuation; RMSD, root-mean-square deviation

## REFERENCES

- (1) Schmidt, A., and Hall, M. N. (1998) Signaling to the actin cytoskeleton. *Annu. Rev. Cell Dev. Biol.* 14, 305–338.
- (2) Luna, E. J., and Hitt, A. L. (1992) Cytoskeleton-plasma membrane interactions. *Science* 258, 955–964.
- (3) Pollard, T. D. (2000) Reflections on a quarter century of research on contractile systems. *Trends Biochem. Sci.* 25, 607–611.
- (4) Heng, Y. W., and Koh, C. G. (2010) Actin cytoskeleton dynamics and the cell division cycle. *Int. J. Biochem. Cell Biol.* 42, 1622–1633.
- (5) Jordan, M. A., and Wilson, L. (1998) Microtubules and actin filaments: dynamic targets for cancer chemotherapy. *Curr. Opin. Cell Biol.* 10 (1), 123–130.
- (6) Jordon, A., Hadfield, J. A., Lawrence, N. J., and McGown, A. T. (1998) Tubulin as a target for anticancer drugs: agents which interact with the mitotic spindle. *Med. Res. Rev.* 4, 259–296.
- (7) Shi, Q., Chen, K., Morris-Natschke, S. L., and Lee, K. H. (1998) Recent progress in the development of tubulin inhibitors as antimitotic antitumor agents. *Curr. Pharm. Des.* 4, 219–248.
- (8) Atencia, R., Asumendi, A., and Garcia-Sanz, M. (2000) Role of cytoskeleton in apoptosis. *Vitam. Horm. (London, U.K.)* 58, 267–297.
- (9) Wu, C., and Dedhar, S. (2001) Integrin-linked kinase (ILK) and its interactors: a new paradigm for the coupling of extracellular matrix to actin cytoskeleton and signaling complexes. *J. Cell Biol.* 155 (4), 505–510.

- (10) Stournaras, C., Stiakaki, E., Koukouritaki, S. B., Theodoropoulos, P. A., Kalmanti, M., Fostinis, Y., and Gravanis, A. (1996) Altered actin polymerization dynamics in various malignant cell types: evidence for differential sensitivity to cytochalasin B. *Biochem. Pharmacol. (Amsterdam, Neth.)* 52 (9), 1339–1346.
- (11) Hemstreet, G. P., Rao, J. Y., Hurst, R. E., Bonner, R. B., Waliszewski, P., Grossman, H. B., Liebert, M., and Bane, B. L. (1996) G-actin as a risk factor and modulatable endpoint for cancer chemoprevention trials. *J. Cell. Biochem.* 25 (Suppl.), 197–204.
- (12) Asch, H. L., Head, K., Dong, Y., Natoli, F., Winston, J. S., Connolly, J. L., and Asch, B. B. (1996) Widespread loss of gelsolin in breast cancers of humans, mice, and rats. *Cancer Res.* 56 (21), 4841–4845.
- (13) Allingham, J. S., Klenchin, V. A., and Rayment, I. (2006) Actin-targeting natural products: structures, properties and mechanisms of action. *Cell. Mol. Life Sci.* 63 (18), 2119–2134.
- (14) Tanenbaum, S. W., Ed. (1978) *Cytochalasins—Biochemical and Cell Biological Aspects*, p 564, North Holland Publishing, Amsterdam, The Netherlands.
- (15) Ayscough, K. R., Stryker, J., Pokala, N., Sanders, M., Crews, P., and Drubin, D. G. (1997) High rates of actin filament turnover in budding yeast and roles for actin in establishment and maintenance of cell polarity revealed using the actin inhibitor latrunculin-A. *J. Cell Biol.* 137 (2), 399–416.
- (16) Dhillon, N., Aggarwal, B. B., Newman, R. A., Wolff, R. A., Kunnumakkara, A. B., Abbruzzese, J. L., Ng, C. S., Badmaev, V., and Kurzrock, R. (2008) Phase II trial of curcumin in patients with advanced pancreatic cancer. *Clin. Cancer Res.* 14, 4491–4499.
- (17) Hatcher, H., Planalp, R., Cho, J., Torti, F. M., and Torti, S. V. (2008) Curcumin: from ancient medicine to current clinical trials. *Cell. Mol. Life Sci.* 65, 1631–1652.
- (18) Aggarwal, B. B., and Sung, B. (2009) Pharmacological basis for the role of curcumin in chronic diseases: an age-old spice with modern targets. *Trends Pharmacol. Sci.* 30, 85–94.
- (19) Aggarwal, B. B., Kumar, A., and Bharti, A. C. (2003) Anticancer potential of curcumin: preclinical and clinical studies. *Anticancer Res.* 23, 363–398.
- (20) Aggarwal, B. B., Sundaram, C., Malani, N., and Ichikawa, H. (2007) Curcumin: the Indian solid gold. *Adv. Exp. Med. Biol.* 595, 1–75.
- (21) Balasubramanian, S., and Eckert, R. L. (2007) Curcumin suppresses AP1 transcription factor-dependent differentiation and activates apoptosis in human epidermal keratinocytes. *J. Biol. Chem.* 282, 6707–6715.
- (22) Aggarwal, B. B., Sethi, G., Ahn, K. S., Sandur, S. K., Pandey, M. K., Kunnumakkara, A. B., Sung, B., and Ichikawa, H. (2006) Targeting signal-transducer-and-activator-of-transcription-3 for prevention and therapy of cancer: modern target but ancient solution. *Ann. N.Y. Acad. Sci.* 1091, 151–169.
- (23) Mackenzie, G. G., Queisser, N., Wolfson, M. L., Fraga, C. G., Adamo, A. M., and Oteiza, P. I. (2008) Curcumin induces cell-arrest and apoptosis in association with the inhibition of constitutively active NF- $\kappa$ B and STAT3 pathways in Hodgkin's lymphoma cells. *Int. J. Cancer* 123, 56–65.
- (24) Chen, Q., Lu, G., Wang, Y., Xu, Y., Zheng, Y., Yan, L., Jiang, Z., Yang, L., Zhan, J., Wu, Y., and Zhou, J. (2009) Cytoskeleton disorganization during apoptosis induced by curcumin in A549 lung adenocarcinoma cells. *Planta Med.* 75 (8), 808–813.
- (25) Holy, J. (2004) Curcumin inhibits cell motility and alters microfilament organization and function in prostate cancer cells. *Cell Motil. Cytoskeleton* 58 (4), 253–268.
- (26) Chakraborti, S., Das, L., Kapoor, N., Das, A., Dwivedi, V., Poddar, A., Chakraborti, G., Janik, M., Basu, G., Panda, D., Chakraborti, P., Suroia, A., and Bhattacharyya, B. (2011) Curcumin recognizes a unique binding site of tubulin. *J. Med. Chem.* 54, 6183–6196.
- (27) Kouyama, T., and Mihashi, K. (1981) Fluorimetry study of N-(1-pyrenyl)iodoacetamide-labelled F-actin. *Eur. J. Biochem.* 114 (1), 33–38.



- (28) Bhattacharyya, B., Kapoor, S., and Panda, D. (2010) Fluorescence spectroscopic methods to analyze drug–tubulin interactions. *Methods Cell Biol.* 95, 301–329.
- (29) Lakowicz, J. R. (1983) *Principles of Fluorescence Spectroscopy*, pp 1–44, Plenum Press, New York.
- (30) Morton, W. M., Ayscough, K. R., and McLaughlin, P. J. (2000) Latrunculin alters the actin-monomer subunit interface to prevent polymerization. *Nat. Cell Biol.* 2 (6), 376–378.
- (31) Eswar, N., Eramian, D., Webb, B., Shen, M. Y., and Sali, A. (2008) Protein structure modeling with MODELLER. *Structural Proteomics*, pp 145–159, Humana Press, New York.
- (32) Morris, G. M., Huey, R., Lindstrom, W., Sanner, M. F., Belew, R. K., Goodsell, D. S., and Olson, A. J. (2009) AutoDock4 and AutoDockTools4: automated docking with selective receptor flexibility. *J. Comput. Chem.* 30 (16), 2785–2791.
- (33) McDonald, I. K., and Thornton, J. M. (1994) Satisfying hydrogen bonding potential in proteins. *J. Mol. Biol.* 238 (5), 777–793.
- (34) Case, D. A., Cheatham, T. E., Darden, T., Gohlke, H., Luo, R., Merz, K. M., Onufriev, A., Simmerling, C., Wang, B., and Woods, R. J. (2005) The Amber biomolecular simulation programs. *J. Comput. Chem.* 26, 1668–1688.
- (35) Gilson, M. K., and Zhou, H. X. (2007) Calculation of protein-ligand binding affinities. *Annu. Rev. Biophys. Biomol. Struct.* 36, 21–42.
- (36) Rastelli, G., Rio, A. D., Degliesposti, G., and Sgobba, M. (2010) Fast and accurate predictions of binding free energies using MM-PBSA and MM-GBSA. *J. Comput. Chem.* 31, 797–810.
- (37) Leung, M. H., and Kee, T. W. (2009) Effective stabilization of curcumin by association to plasma proteins: human serum albumin and fibrinogen. *Langmuir* 25, 5773–5777.
- (38) Wang, Y. J., Pan, M. H., Cheng, A. L., Lin, L. I., Ho, Y. S., Hsieh, C. Y., and Lin, J. K. (1997) Stability of curcumin in buffer solutions and characterization of its degradation products. *J. Pharm. Biomed. Anal.* 15 (12), 1867–1876.
- (39) Chakraborti, S., Dhar, G., Dwivedi, V., Das, A., Poddar, A., Chakraborti, G., Basu, G., Chakrabarti, P., Surolia, A., and Bhattacharyya, B. (2013) Stable and potent analogues derived from the modification of the dicarbonyl moiety of curcumin. *Biochemistry* 52 (42), 7449–7460.
- (40) Freire, E. (2008) Do enthalpy and entropy distinguish first in class from best in class? *Drug Discovery Today* 13, 869–874.
- (41) Kashman, Y., Groweiss, A., and Shmueli, A. (1980) Latrunculin, a new 2-thiazolidinone macrolide from the marine sponge *Latrunculia magnifica*. *Tetrahedron Lett.* 21, 3629–3632.
- (42) Allingham, J. S., Klenchin, V. A., and Rayment, I. (2006) Actin-targeting natural products: structures, properties and mechanisms of action. *Cell. Mol. Life Sci.* 63 (18), 2119–2134.
- (43) Fenteany, G., and Zhu, S. (2003) Small-molecule inhibitors of actin dynamics and cell motility. *Curr. Top. Med. Chem.* 3 (6), 593–616.
- (44) Goddette, D. W., and Frieden, C. (1986) Actin polymerization. The mechanism of action of cytochalasin D. *J. Biol. Chem.* 261 (34), 15974–15980.
- (45) Nair, U. B., Joel, P. B., Wan, Q., Lowey, S., Rould, M. A., and Trybus, K. M. (2008) Crystal structures of monomeric actin bound to cytochalasin D. *J. Mol. Biol.* 384 (4), 848–864.
- (46) Khaitlina, S. Y., and Strzelecka-Golaszewska, H. (2002) Role of the DNase-I-binding loop in dynamic properties of actin filament. *Biophys. J.* 82 (1), 321–334.
- (47) Kim, E., and Reisler, E. (1996) Intermolecular coupling between loop 38–52 and the C-terminus in actin filaments. *Biophys. J.* 71 (4), 1914–1919.
- (48) Galkin, V. E., Orlova, A., Schröder, G. F., and Egelman, E. H. (2010) Structural polymorphism in F-actin. *Nat. Struct. Mol. Biol.* 17 (11), 1318–1323.
- (49) Marcu, M. G., Jung, Y. J., Lee, S., Chung, E. J., Lee, M. J., Trepel, J., and Neckers, L. (2006) Curcumin is an inhibitor of p300 histone acetyltransferase. *Med. Chem.* 2 (2), 169–174.
- (50) Majhi, A., Rahman, G. M., Panchal, S., and Das, J. (2010) Binding of curcumin and its long chain derivatives to the activator binding domain of novel protein kinase C. *Bioorg. Med. Chem.* 18 (4), 1591–1598.
- (51) Fang, J., Lu, J., and Holmgren, A. (2005) Thioredoxin reductase is irreversibly modified by curcumin: a novel molecular mechanism for its anticancer activity. *J. Biol. Chem.* 280 (26), 25284–25290.
- (52) Sahu, A., Kasoju, N., and Bora, U. (2008) Fluorescence study of the curcumin–casein micelle complexation and its application as a drug nanocarrier to cancer cells. *Biomacromolecules* 9 (10), 2905–2912.
- (53) Sethi, G., Sung, B., Kunnumakkara, A. B., and Aggarwal, B. B. (2009) Targeting TNF for treatment of cancer and autoimmunity. In *Therapeutic Targets of the TNF Superfamily*, pp 37–51, Springer, New York.
- (54) Sahoo, B. K., Ghosh, K. S., Bera, R., and Dasgupta, S. (2008) Studies on the interaction of diacetylcurcumin with calf thymus-DNA. *Chem. Phys.* 351 (1), 163–169.
- (55) Nafisi, S., Adelzadeh, M., Norouzi, Z., and Sarbolouki, M. N. (2009) Curcumin binding to DNA and RNA. *DNA Cell Biol.* 28 (4), 201–208.
- (56) Gupta, K. K., Bharne, S. S., Rathinasamy, K., Naik, N. R., and Panda, D. (2006) Dietary antioxidant curcumin inhibits microtubule assembly through tubulin binding. *FEBS J.* 273 (23), 5320–5332.
- (57) Rai, D., Singh, J., Roy, N., and Panda, D. (2008) Curcumin inhibits PtsZ assembly: an attractive mechanism for its antibacterial activity. *Biochem. J.* 410, 147–155.
- (58) Ahmad, B., and Lapidus, L. J. (2012) Curcumin prevents aggregation in  $\alpha$ -synuclein by increasing reconfiguration rate. *J. Biol. Chem.* 287 (12), 9193–9199.
- (59) Reinke, A. A., and Gestwicki, J. E. (2007) Structure–activity relationships of amyloid beta-aggregation inhibitors based on curcumin: influence of linker length and flexibility. *Chem. Biol. Drug Des.* 70 (3), 206–215.